TPX2 is required for postmitotic nuclear assembly in cell-free *Xenopus laevis* egg extracts

Lori L. O'Brien and Christiane Wiese

Department of Biochemistry, University of Wisconsin–Madison, Madison, WI 53706

Cell division in many metazoa is accompanied by the disassembly of the nuclear envelope and the assembly of the mitotic spindle. These dramatic structural rearrangements are reversed after mitosis, when the mitotic spindle is dismantled and the nuclear envelope reassembles. The targeting protein for XKlp2 (TPX2) plays important roles in mitotic spindle assembly. We report that TPX2 depletion from nuclear assembly extracts prepared from *Xenopus laevis* eggs results in the formation of nuclei that are only about one fifth the size of control nuclei. TPX2-depleted nuclei assemble nuclear envelopes, nuclear pore complexes, and a lamina, and they perform nuclear-specific functions, including DNA replication. We show that TPX2 interacts with lamina-associated polypeptide 2 (LAP2), a protein known to be required for nuclear assembly in interphase extracts and in vitro. LAP2 localization is disrupted in TPX2-depleted nuclei, suggesting that the interaction between TPX2 and LAP2 is required for postmitotic nuclear reformation.

Introduction

The defining feature of eukaryotic cells is the separation of the chromosomes from the cytoplasm, which is achieved by the nuclear envelope (NE), a highly selectively permeable double membrane system. The enclosure of the genetic information within the nucleus generates a unique environment that separates DNA replication, transcription, and RNA processing from protein synthesis (for reviews see Shumaker et al., 2003; Gruenbaum et al., 2005). Communication between the nucleus and the cytoplasm occurs through nuclear pore complexes (NPCs), specialized protein-filled "holes" that span the NE. The NE of eukaryotes consists of a double lipid bilayer named the inner and outer nuclear membranes. The outer nuclear membrane is structurally and functionally continuous with the ER, whereas the inner nuclear membrane harbors a unique set of proteins that helps connect the membrane to the underlying lamina and provide specialized chromatin regulatory domains (Schirmer et al., 2003; for reviews see Holmer and Worman, 2001; Goldman et al., 2002; Maidment and Ellis, 2002; Gruenbaum et al., 2003; Schirmer and Gerace, 2005). The inner nuclear membrane is anchored to the nuclear lamina, a polymeric meshwork composed of specialized intermediate filament proteins named lamins. The major lamin type present in *Xenopus laevis* eggs, lamin B3, is associated with the inner nuclear membrane via posttranslational isoprenyl groups (for review see Goldman et al., 2002) as well as integral inner nuclear membrane and lamina-associated polypeptides (LAPs; for reviews see Gant and Wilson, 1997; Shumaker et al., 2003; Gruenbaum et al., 2005). The nuclear lamina provides structural support to the nucleus (Newport et al., 1990), and its expansion is required for continued nuclear growth (Lopez-Soler et al., 2001; Shumaker et al., 2005).

During cell division in metazoa, NE components are disassembled and dispersed throughout the dividing cell (Gerace and Blobel, 1980; for review see Gant and Wilson, 1997). After NE breakdown, the mitotic spindle assembles and then segregates the duplicated chromosomes. At the end of mitosis, the mitotic spindle disassembles and a new NE reassembles around the segregated chromosomes. Postmitotic nuclear reassembly requires at least two distinguishable steps: (1) enclosure of the chromatin within a functional NE and (2) growth and expansion of this NE. Initial steps during enclosure of the chromatin include the targeting of nuclear vesicles to the chromosomes, the fusion of vesicles to reform the nuclear membranes, the assembly of NPCs, and the formation of the nuclear lamina. Continued NE growth requires further vesicle fusion, nuclear protein import, and lamina expansion (for reviews see Gant and Wilson, 1997; Marshall and Wilson, 1997). Although it is clear that phosphorylation and dephosphorylation of key structural elements are required for the large-scale molecular rearrangements that take place during

Correspondence to Christiane Wiese: wiese@biochem.wisc.edu

Abbreviations used in this paper: DHCC, 3,3′-dihexyloxacarbocyanine; IIF, indirect immunofluorescence; LAP, lamina-associated polypeptide; NE, nuclear envelope; NPC, nuclear pore complex.

The online version of this article contains supplemental material.

The Journal of Cell Biology, Vol. 173, No. 5, June 5, 2006 685–694
http://www.jcb.org/cgi/doi/10.1083/jcb.200512107

NE breakdown and reformation, the molecular mechanisms of these processes remain largely unknown.

One class of proteins implicated in NE reformation is LAPs. LAP2β (also known as thymopoietin) is a ubiquitously expressed and highly conserved (Zevin-Sonkin et al., 1992; Harris et al., 1994, 1995; Berger et al., 1996; Ishijima et al., 1996; Theodor et al., 1997) inner nuclear membrane protein that binds to lamin B and chromosomes (Foisner and Gerace, 1993; Furukawa et al., 1995, 1998). The six isoforms of mammalian LAP2 (designated α, β, γ, δ, ε, and ζ) are generated by alternative splicing of the same transcript (Harris et al., 1994; Berger et al., 1996; Dechat et al., 1998). With the exception of mammalian LAP2α and LAP2ζ, all LAP2 isoforms have a common transmembrane domain at their COOH terminus and are type II integral membrane proteins of the inner nuclear membrane (for review see Dechat et al., 2000). LAP2γ, δ, and ε are closely related to LAP2β, but each lacks one or more of several short regions of the nucleoplasmically oriented NH_2-terminal domain, which is involved in both lamin B and chromatin binding. In mammals, LAP2α, β, and γ are the major LAP2 isoforms (Harris et al., 1994; Alsheimer et al., 1998; Goldberg et al., 1999). Several LAP2 isoforms have also been found in *X. laevis* tissue culture cells (Lang et al., 1999), oocytes (Gant et al., 1999; Lang et al., 1999), or early embryos (Lang et al., 1999), but their molecular structure has not been elucidated. The three LAP2 cDNAs isolated from *X. laevis* oocyte mRNAs (coding for proteins with predicted molecular masses of 62.84 kD [clone 2], 46.4 kD [clone 3], and 58.7 kD [clone 4]) most closely resemble human LAP2β in primary sequence and also appear to be related by alternative splicing (Gant et al., 1999), but how these clones correspond to the ∼85-kD oocyte-specific LAP2 isoform (Lang et al., 1999) is presently unclear. It is interesting to note that its biochemical properties make it likely that the 85-kD isoform has a transmembrane domain and is therefore related to LAP2β (Lang et al., 1999).

LAP2β is proposed to link chromatin to the NE during interphase (Foisner and Gerace, 1993; Furukawa et al., 1995, 1998), and at least two lines of evidence support the notion that LAP2β is required for NE reassembly and expansion after cell division: (1) microinjection of recombinant LAP2 mutant proteins into mammalian cells inhibits postmitotic nuclear expansion (Yang et al., 1997) and (2) addition of recombinant LAP2 mutant proteins to *X. laevis* egg extracts disrupts nuclear morphology and lamina assembly (Gant et al., 1999).

In recent years, an increasing number of proteins have been shown to play important and sometimes seemingly unrelated roles in both interphase and mitosis (for review see Kline-Smith and Walczak, 2004). Most prominent among them are the components of the nuclear trafficking machinery, the RanGTPase, and its binding proteins and effectors (for reviews see Quimby and Dasso, 2003; Di Fiore et al., 2004; Hetzer et al., 2005). Several spindle assembly factors are mitotic targets of the RanGTPase pathway, including the targeting protein for XKlp2 (TPX2). TPX2 was originally discovered as a microtubule binding and loading factor for the mitotic kinesin XKlp2 (Wittmann et al., 2000). Since then, it has been shown to play multiple roles during mitosis: TPX2 is involved in focusing microtubules at mitotic spindle poles (Wittmann et al., 2000), in bipolar mitotic spindle assembly (Garrett et al., 2002; Gruss et al., 2002), in nucleating microtubules near the chromosomes (Gruss et al., 2001; Schatz et al., 2003), and in activating the mitotic kinase Eg2 in a RanGTPase-dependent manner (Tsai et al., 2003; Eyers and Maller, 2004). TPX2 localizes predominantly to spindle poles during mitosis and to the nucleus during interphase (Garrett et al., 2002; Wittmann et al., 2000). Although important functions for TPX2 in mitotic spindle assembly are well documented (Wittmann et al., 2000; for review see Gruss and Vernos, 2004), a functional role for its accumulation in the nucleus during interphase has not been reported.

We show that *X. laevis* TPX2 interacts with LAP2 in a cell-free nuclear assembly assay based on extracts made from the eggs of the South African clawed frog, *X. laevis,* and in vitro. When interphase *X. laevis* egg extracts depleted of TPX2 were induced to assemble nuclei by the addition of demembranated sperm chromatin, they formed significantly smaller nuclei than control extracts. Nonetheless, these nuclei were able to perform nuclear functions, including nuclear import, selective permeability, and DNA replication. TPX2 depletion resulted in decreased accumulation of LAP2 at the NE. Together, these data suggest a novel role for TPX2 in LAP2-mediated NE growth.

Results

TPX2 depletion from interphase *X. laevis* egg extracts results in small, misshapen nuclei

TPX2 accumulates in nuclei assembled in vitro (Wittmann et al., 2000) and in interphase tissue culture cells (Fig. 1 A; Wittmann et al., 2000; Garrett et al., 2002; Gruss et al., 2002; Stewart and Fang, 2005). TPX2 staining appears mostly reticular but also shows a distinct nuclear rim staining in a subset of nuclei (Fig. 1 A; see Fig. 5 in Wittmann et al., 2000). Two explanations can account for the accumulation of TPX2 in nuclei: (1) TPX2 needs to be sequestered from the cytoplasm during interphase to avoid its effects on microtubules or (2) TPX2 plays a functional role in interphase nuclear assembly or architecture. The reticular distribution and nuclear rim staining of TPX2 prompted us to further explore whether TPX2 might serve a functional role in the nucleus.

Nuclear assembly can be studied in vitro using well-established nuclear assembly assays based on extracts made from the eggs of the South African clawed frog, *X. laevis*. In a process that mimics sperm entry during fertilization, demembranated *X. laevis* sperm added to interphase extracts readily attract NE components and assemble functional nuclei in vitro (for review see Marshall and Wilson, 1997). To test whether TPX2 has a role in nuclear assembly or architecture, we used the in vitro nuclear assembly assay to examine the effects on nuclear assembly of altering TPX2 levels (Fig. 1). Adding bacterially expressed recombinant TPX2 to interphase extracts resulted in a dose-dependent reduction in the size of nuclei formed around exogenously added sperm chromatin (Fig. 1 B). Similarly, depletion of TPX2 from the egg extract resulted in the formation of small nuclei (Fig. 1 C; we refer to these as TPX2-Δ nuclei),

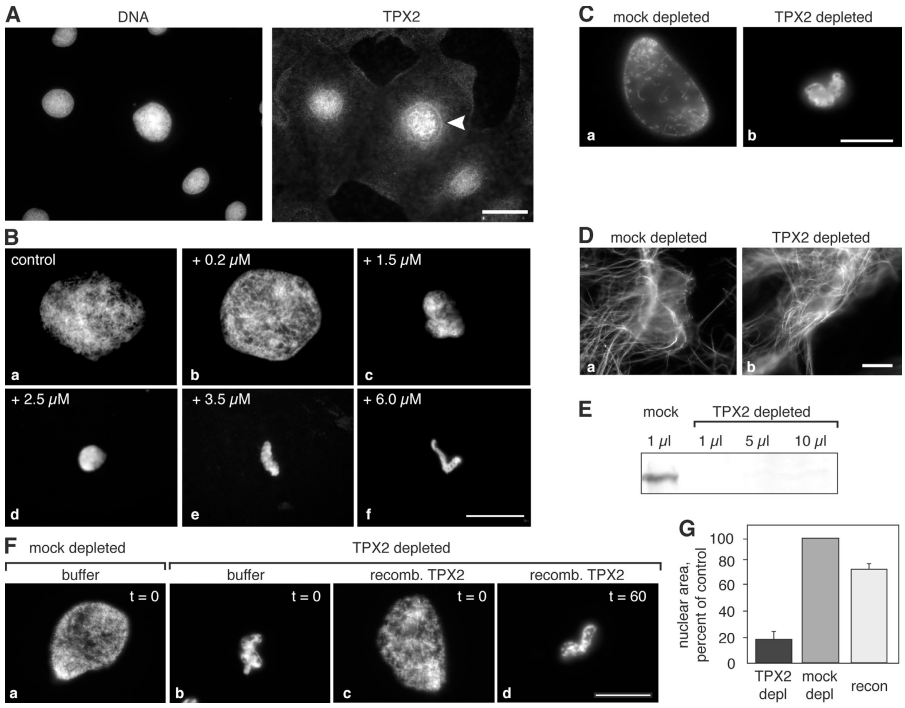

Figure 1. **Disrupting the levels of TPX2 in interphase extracts affects nuclear size.** (A) TPX2 immunofluorescence in *X. laevis* tissue culture cells. A typical microscope field with several interphase cells stained for DNA (a) or TPX2 (b) is shown. The arrowhead denotes a cell in which TPX2 localizes to the nuclear rim. (B) Addition of exogenous TPX2 to interphase extracts disrupts nuclear size. Nuclear assembly reactions were supplemented with buffer (a), or 0.2 μM (b), 1.5 μM (c), 2.5 μM (d), 3.5 μM (e), or 6 μM (f) recombinant TPX2, incubated for 80 min at room temperature, fixed, spun onto coverslips, and stained for DNA with Hoechst dye. The concentration of TPX2 added ranged from twofold (0.2 μM) to 60-fold (6 μM) over endogenous TPX2 levels. (C) Interphase *X. laevis* egg extracts were depleted with either nonspecific IgG (a) or anti-TPX2 antibodies (b). The extracts were then induced to form nuclei by addition of demembranated *X. laevis* sperm chromatin, incubated at room temperature for 80 min, fixed, and spun onto coverslips. The coverslips were stained with Hoechst dye to visualize the DNA. (D) Samples were prepared as in C, but were supplemented with a small amount of rhodamine-labeled tubulin to visualize microtubule structures in mock-depleted (a) or TPX2-Δ (b) extracts. (E) TPX2 levels are reduced by >98% in depleted extracts. TPX2 Western blot of mock-depleted (lane 1) or increasing amounts of TPX2-Δ (lanes 2–4) extracts. The volume of extract loaded ranged from 1 to 10 μl for the depleted extract as indicated above the lanes. (F) Nuclear size can be rescued by readdition of bacterially expressed recombinant TPX2, but TPX2 must be present at the start of the assembly reaction. Nuclei are visualized by DNA staining. Typical nuclei assembled in mock-depleted extract (a), TPX2-Δ extract supplemented with buffer (b), TPX2-Δ extract supplemented with 100 nM TPX2 at the beginning of the assembly reaction (c), or TPX2-Δ extract supplemented with 100 nM TPX2 60 min after the beginning of the assembly reaction and incubated for an additional 60 min (d) are shown. Buffer controls were supplemented with an equivalent volume of buffer. (G) Quantitation of the area enclosed by the nuclei assembled in mock-depleted extracts, TPX2-Δ extracts, or extracts reconstituted with TPX2 at the beginning of the assembly reaction, as described for the experiment shown in F. At least 50 nuclei were measured per sample in five independent experiments. Error bars indicate standard deviation. Bars, 25 μm.

whereas it had no effect on microtubules (Fig. 1 D). Under conditions where >98% of TPX2 was depleted from the extract (Fig. 1 E) and nuclei were fixed and examined 80 min after the start of the assembly reaction, nuclear size was reduced by ~80% compared with controls (Fig. 1, F and G). Importantly, readdition of endogenous levels (~100 nM; Wittmann et al., 2000) of recombinant TPX2 to TPX2-Δ extract largely rescued the defects in nuclear size (Fig. 1, F and G), but only if the exogenous TPX2 was supplied at the beginning of the reaction. Addition of recombinant TPX2 1 h after the start of the nuclear assembly reaction was unable to rescue the defect even after prolonged (>60 min) incubation (Fig. 1, F and G). These results suggested that both too much and too little TPX2 disrupted nuclear assembly. They further suggested that TPX2 function is required during the early stages of nuclear reformation.

TPX2-Δ nuclei assemble fully functional NEs that support replication

Several possibilities could account for the small size of TPX2-Δ nuclei. For example, TPX2 depletion could directly or indirectly influence the levels of one or more nuclear components that are limiting. These include the building blocks of the nuclear membranes, the nuclear lamina, or the NPCs or factors involved in chromatin remodeling during decondensation. It was also possible that nuclear import was somehow affected. Alternatively, TPX2 could be involved in the overall regulation of nuclear assembly. Furthermore, importin α and β have been implicated in nuclear membrane fusion and NPC assembly (Askjaer et al., 2002; Harel et al., 2003; Ryan et al., 2003; Walther et al., 2003; Hachet et al., 2004; for review see Hetzer et al., 2005), and TPX2 is known to interact with both (Gruss et al., 2001; Schatz et al., 2003).

To distinguish these possibilities and to begin to understand the function of TPX2 in nuclear assembly, we examined nuclei assembled in TPX2-Δ extracts for their ability to support chromatin decondensation and to assemble nuclear membranes and NPCs. Because small nuclei could result from chromatin decondensation defects, we first examined the effect of TPX2 depletion on stage I chromatin decondensation (as defined by Philpott et al., 1991). Both the extent and the timing of decondensation of chromatin incubated in high-speed supernatant depleted of TPX2 were indistinguishable from mock-depleted extracts (Fig. S1, available at http://www.jcb.org/cgi/content/full/jcb.200512107/DC1), suggesting that TPX2 was not required for the initial stages of chromatin decondensation. Next, we tested whether TPX2-Δ nuclei were able to assemble nuclear membranes. Staining of TPX2-Δ nuclei with the membrane dye 3,3′-dihexyloxacarbocyanine (DHCC) revealed a smooth and continuous line (Fig. 2 A), suggesting fused and fully assembled nuclear membranes (Boman et al., 1992; Harel et al., 2003).

To address whether TPX2-Δ nuclei possessed NPCs and a nuclear lamina, we immunostained nuclei assembled in TPX2-Δ

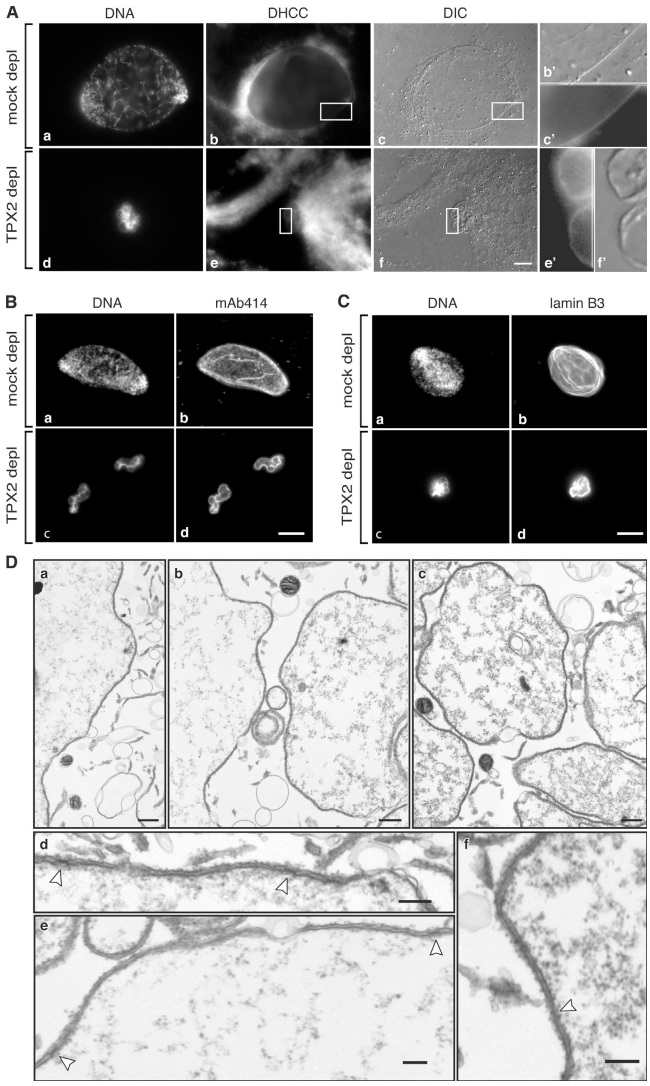

Figure 2. **TPX2-Δ nuclei have nuclear membranes, NPCs, and a lamina.** (A) Nuclei assembled in mock (a–c) or TPX2-Δ (d–f) extracts were stained for DNA with Hoechst dye (a and d) or for membranes with DHCC (b and e) or were visualized by Nomarski (DIC) optics (c and f). (b′, c′, e′, and f′) Higher magnification views of the areas indicated by white rectangles in b, c, e, and f, respectively. (B) TPX2-Δ nuclei stain positively for the NPC probe, mAb414. Nuclei were assembled in mock-depleted (a and b) or TPX2-Δ (c and d) extracts, fixed, and spun onto coverslips. Nuclei were then processed for immunofluorescence with mAb414 (b and d) and for DNA staining with Hoechst dye (a and c). (C) TPX2-Δ nuclei assemble a nuclear lamina. Nuclei were prepared as in B and were stained for lamin B3 (b and d) or DNA (a and c). (D) Thin-section electron micrographs of untreated (a and d), TPX2-Δ (b and e), or mock-depleted (c and f) nuclei. Lower magnifications (a–c) reveal the overall appearance of the nuclei. Higher magnifications (d–f) reveal double nuclear membranes and NPCs (arrowheads). Bars: (A, B, and C) 25 μm; (D, a–c) 500 nm; (D, d–f) 200 nm.

extracts for nucleoporins using the monoclonal antibody mAb414 (Davis and Blobel, 1986) or for lamin B3 using the monoclonal antibody L6-5D5 (Stick, 1988). MAb414 robustly labeled the nuclei assembled in TPX2-Δ extracts, indicating the presence of NPCs (Fig. 2 B and Fig. S2, available at http://www.jcb.org/cgi/content/full/jcb.200512107/DC1). Similarly, anti-lamin antibody robustly labeled TPX2-Δ nuclei, indicating the presence of a lamina (Fig. 2 C). Consistent with these observations, thin-section electron microscopy of TPX2-Δ nuclei revealed NPCs embedded in a double nuclear membrane (Fig. 2 D, b and e) that were indistinguishable from untreated (Fig. 2 D, a and d) or mock-depleted (Fig. 2 D, c and f) controls. Interestingly, the overall ultrastructure of TPX2-Δ nuclei was also indistinguishable from controls (Fig. 2 D).

It was possible that, even though NE membranes and NPCs could assemble around chromatin in TPX2-Δ extracts, the resulting structures were unable to perform typical nuclear functions, such as nuclear protein import, exclusion of nonnuclear substrates, and DNA replication. To address these questions, we first added rhodamine-labeled nucleoplasmin (Newmeyer and Wilson, 1991) to TPX2-Δ nuclear assembly reactions. Overlap of the rhodamine signal with the chromatin stain indicated that the labeled nucleoplasmin was imported into the depleted nuclei (Fig. 3 A). When nuclear protein import was experimentally blocked by the addition of the inhibitor wheat germ agglutinin (Finlay et al., 1987) rhodamine nucleoplasmin failed to accumulate in the nuclei (Fig. 3 A). These results suggested that TPX2-Δ nuclei are competent for nuclear import.

To determine whether TPX2-Δ nuclei provided a permeability barrier, rhodamine-labeled 155-kD dextran was added to TPX2-Δ nuclear assembly reactions. The dextran was excluded from TPX2-Δ nuclei (Fig. 3 B), indicating that they were able to selectively exclude nonnuclear compounds. Next, we sought to determine whether TPX2-Δ nuclei were competent for DNA replication. To test replication efficiency, we incubated depleted extracts with [^{32}P]dCTP and measured the amount of incorporation of the label. The TPX2-Δ nuclei were able to incorporate [^{32}P]dCTP (Fig. 3 C). To distinguish DNA repair from DNA replication, we measured [^{32}P]dCTP incorporation in the presence of the inhibitor of DNA polymerase α, aphidicolin. Incorporation of labeled dCTP was sensitive to aphidicolin (Fig. 3 C, a), indicating that it was not caused by DNA repair. Thus, we conclude that TPX2 is not required for DNA replication. Interestingly, in some experiments, replication proceeded more efficiently in TPX2-Δ nuclei compared with mock-depleted controls (Fig. 3, C and D). This is discussed in more detail in the Discussion section.

In summary, we concluded that, despite their small size, nuclei assembled in TPX2-Δ interphase extracts were able to assemble a double nuclear membrane that contained functional NPCs and a nuclear lamina. We further concluded that TPX2-Δ nuclei were able to perform functions generally ascribed to nuclei, such as selective nuclear import and DNA replication.

LAP2 is a binding partner of TPX2 in interphase

To identify potential binding partners of TPX2 during nuclear assembly and thus begin to understand how TPX2 functions in nuclear assembly, we analyzed GST-TPX2 pull downs from interphase or mitotic *X. laevis* egg extracts. SDS-PAGE and Coomassie staining showed that several proteins copurified with GST-TPX2 incubated in interphase or mitotic extracts and reisolated (Fig. 4 A). MALDI-TOF (matrix-assisted laser desorption ionization–time of flight) mass spectrometry analysis of the ∼40-kD protein that copurified with GST-TPX2

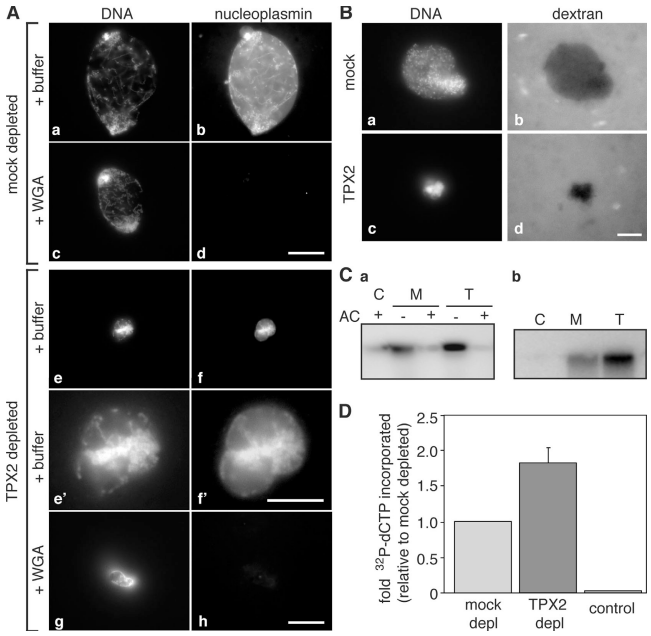

Figure 3. **TPX2-Δ nuclei form fully functional NEs.** (A) TPX2-Δ nuclei import a nuclear substrate. Mock-depleted (a–d) or TPX2-Δ (e–h) nuclear assembly reactions were supplemented with rhodamine-labeled nucleoplasmin to assay nuclear import. To distinguish import from nonspecific association of nucleoplasmin with the nuclei, some reactions (c, d, g, and h) were supplemented with the inhibitor of nuclear import, wheat germ agglutinin (WGA). Nuclei were visualized by DNA stain (a, c, e, e', and g) or rhodamine fluorescence (b, d, f, f', and h). (e' and f') Higher magnification views of e and f, respectively. (B) TPX2-Δ nuclei exclude a nonnuclear substance. Mock-depleted (a and b) or TPX2-Δ (c and d) nuclear assembly reactions were spiked with rhodamine-labeled 155-kD dextran, and a small amount of the reaction was spotted onto a coverslip. Nuclei were visualized by Hoechst staining (a and c) and the dextran by fluorescence (b and d). (C) TPX2-Δ nuclei replicate their DNA. Autoradiographs of two representative replication assays are shown. [^{32}P]dCTP was added to control (C), mock-depleted (M), or TPX2-Δ (T) extracts supplemented with ~100 sperm chromatin/microliter, and the reactions were incubated for 3 h at room temperature to allow DNA replication. Reactions were then stopped, separated on a 0.8% agarose gel, and visualized by autoradiography. Two types of control extracts were used, with similar results: (a) duplicate reactions were treated with the inhibitor of replication, aphidicolin (AC); (b) [^{32}P]dCTP was added to mitotic extracts. (D) Quantitation of DNA replication in four independent experiments, normalized to the amount of label incorporated in the mock-depleted controls. Error bars indicate standard deviation. Bars: (A [a–f, g, and h] and B) 25 μm; (A, e' and f') 10 μm.

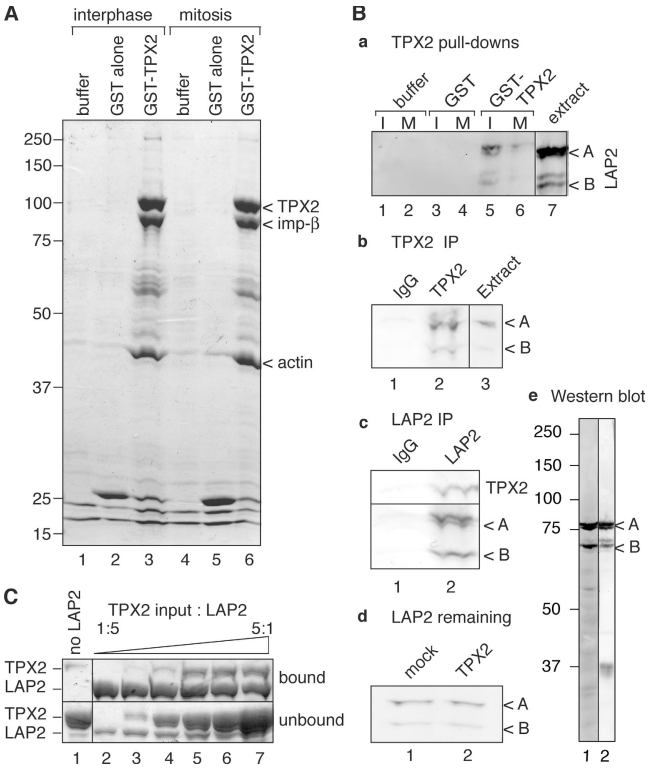

Figure 4. **TPX2 interacts with LAP2.** (A) Coomassie-stained SDS-PAGE gel of proteins that copurify with GST-TPX2 from interphase or mitotic extracts. GST-TPX2, GST, or buffer were incubated in interphase or mitotic extracts and were retrieved using glutathione-agarose beads. Proteins were eluted from the beads by treatment with a protease that cuts between the GST and TPX2 (the GST remains bound to the beads), and eluted proteins were boiled in SDS sample buffer and separated on a 10% gel. Sizes of molecular mass markers are indicated on the left, and the position of TPX2, importin β, and actin are indicated on the right. (B, a) LAP2 associates with GST-TPX2 reisolated from egg extracts. LAP2 Western blots of GST pull downs from interphase and mitosis, prepared as in A. Buffer, GST, or GST-TPX2 was added to interphase or mitotic extract. (b) LAP2 coimmunoprecipitates with TPX2. LAP2 Western blot of proteins that coimmunoprecipitate with TPX2. Lane 1 shows IgG control, lane 2 shows TPX2 immunoprecipitation, and lane 3 shows extract control. (c) TPX2 (top) or LAP2 (bottom) Western blots of proteins that coimmunoprecipitate with LAP2. Lane 1 shows IgG control, and lane 2 shows LAP2 immunoprecipitation. The positions of TPX2 and LAP2 are indicated on the right. (d) LAP2 is not codepleted in extracts depleted of TPX2. LAP2 Western blot of extracts immunodepleted with control or TPX2 antibodies. (e) Western blot of *X. laevis* egg extracts probed with LAP2 antibodies. Two doublets (A and B) are recognized by two different antibodies raised against *X. laevis* LAP2. (C) LAP2 interacts with TPX2 in vitro. Bacterially expressed GST-XLAP2 was incubated in vitro with increasing amounts of untagged TPX2 (lanes 2–7). GST-LAP2 was then retrieved with glutathione-agarose beads, and the amount of TPX2 that copurified (top) was examined on Coomassie-stained SDS-PAGE gels and compared with the amount that remained in the supernatant (bottom). Lane 1 shows TPX2 incubated with beads in the absence of GST-XLAP2. The positions of TPX2 and LAP2 are indicated on the left of each panel.

(excised from the gel and processed for mass spectrometry as described in Materials and methods) identified two proteins that were of special interest to us: actin and the inner nuclear membrane protein LAP2. Further analysis by Western blots revealed that both actin (unpublished data) and LAP2 (two isoforms migrating at ~85 and ~60 kD, respectively) were indeed present in the TPX2 pull downs (Fig. 4 B, a and e).

Although no obvious differences between interphase and mitotic pull downs were apparent by Coomassie staining, Western blots revealed that LAP2 preferentially copurified with GST-TPX2 incubated in interphase extracts (Fig. 4 B, a). Endogenous LAP2 and TPX2 also interacted, as shown by coimmunoprecipitation experiments using either TPX2 or LAP2 antibodies as probes (Fig. 4 B, b and c).

To determine whether the interaction between TPX2 and LAP2 was direct or possibly mediated by another protein, purified recombinant GST-XLAP2 nucleoplasmic domain (amino acids 1–471) was mixed with increasing amounts of untagged recombinant TPX2, and the mixture was incubated in vitro. Proteins were then adsorbed to glutathione-agarose beads, and bound and unbound proteins were separated by SDS-PAGE and visualized by Coomassie staining (Fig. 4 C). TPX2 binding to GST-LAP2 was specific and saturable (Fig. 4 C), suggesting that LAP2 directly bound to TPX2.

If TPX2 and LAP2 interact in vivo, they would be expected to colocalize at least during some parts of the cell cycle. To assess protein distribution, TPX2 and LAP2 were localized in *X. laevis* tissue culture. Double stain immunofluorescence microscopy showed that TPX2 and LAP2 overlapped at the nuclear rim in a subset of interphase cells and especially during telophase and early G1 (Fig. 5). These results are consistent with the idea that TPX2 and LAP2 function together during nuclear reformation.

TPX2 is required for nuclear accumulation of LAP2

LAP2 is involved in attaching nuclear membranes to the underlying lamina and chromatin, and its disruption results in nuclear growth defects (Yang et al., 1997; Gant et al., 1999). These defects are remarkably similar to the defects observed in TPX2-Δ extracts. We therefore wondered whether the interaction between LAP2 and TPX2 is important for nuclear assembly. To test this hypothesis, we monitored LAP2 localization in TPX2-Δ nuclei. Immunofluorescence revealed that LAP2 localized mainly to the nuclear rim during the early stages of nuclear assembly in mock-depleted extracts and to punctate structures at later stages (Fig. 6 A, a) but was distributed more diffusely throughout the nuclei at all stages in TPX2-Δ extracts (Fig. 6 A, b, and Fig. S3, available at http://www.jcb.org/cgi/content/full/jcb.200512107/DC1). There also was an overall reduction in the amount of LAP2 associated with TPX2-Δ nuclei. To test whether mislocalization was specific to LAP2 or a more general phenomenon, nuclei were also stained for lamin B3 or for NPC components using mAb414 (Fig. S2). Taking into account the differences in shape and size of TPX2-Δ and mock-depleted nuclei, both lamina and NPC assembly appeared qualitatively similar in TPX2-Δ extracts compared with mock-depleted extracts (Fig. S2). Similarly, TPX2 localization seemed unaffected by the addition of bacterially expressed human $LAP2_{1–408}$ to nuclear assembly reactions (Fig. 6 B), a condition that disrupts endogenous LAP2 function (Gant et al., 1999). Together, these results suggest that TPX2 is required for LAP2 localization and that this activity of TPX2 is required for proper nuclear assembly.

Discussion

TPX2 has well-documented functions in mitotic spindle assembly and in the formation of microtubules near the chromosomes (for review see Gruss and Vernos, 2004), although the molecular

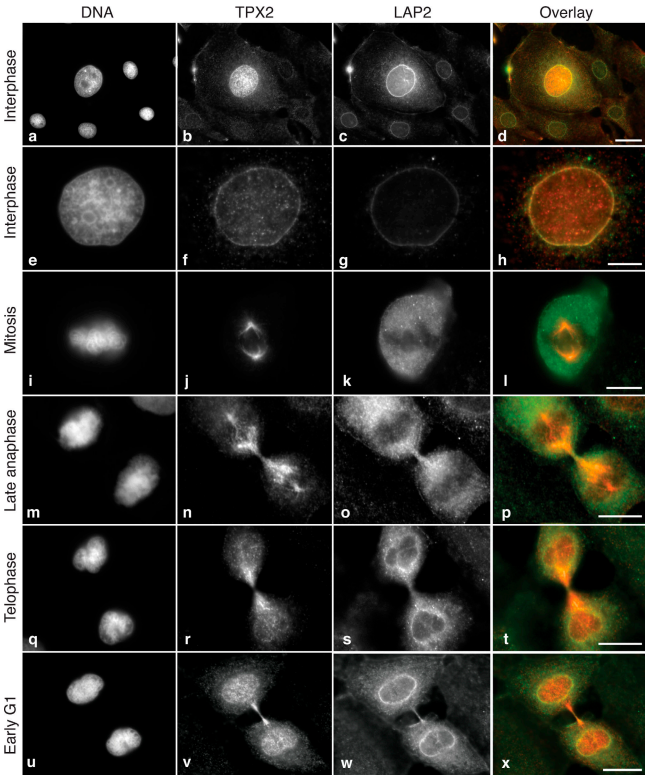

Figure 5. **TPX2 and LAP2 colocalize at the nuclear rim during interphase in *X. laevis* tissue culture cells.** *X. laevis* tissue culture cells triple stained for TPX2 (green), LAP2 (red), and DNA. (a–d) A field containing several interphase cells; (e–h) higher magnification of an individual interphase cell; (i–l) metaphase; (m–p) late anaphase; (q–t) telophase; (u–x) early G1. Bars: (d) 25 μm; (h, l, p, t, and x) 10 μm.

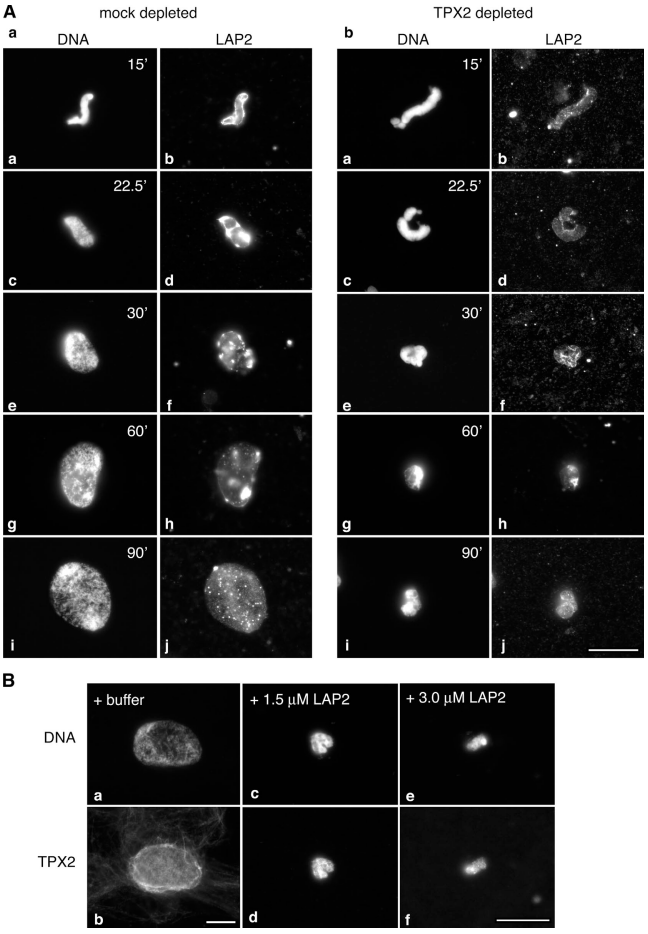

Figure 6. **TPX2 depletion disrupts LAP2 accumulation in nuclei.** (A) LAP2 IIF in mock-depleted (a) or TPX2-Δ (b) nuclei fixed at various times after initiating nuclear assembly. (a, c, e, g, and i) Stained for DNA; (b, d, f, h, and j) stained for LAP2. Time (in minutes) is indicated in the top right corner of the DNA panels. (B) TPX2 IIF (b, d, and f) of nuclei assembled in reactions supplemented with buffer (a and b), 1.5 μM recombinant LAP2 (c and d), or 3.0 μM recombinant LAP2 (e and f). Nuclei were stained with Hoechst dye (a, c, and e) to visualize the DNA. Bars, 25 μm.

mechanisms by which it carries out these functions remain obscure. Consistent with its role in spindle assembly, TPX2 localizes to the spindle poles in mitosis, and a variety of mitotic binding partners for TPX2 have been described (Wittmann et al., 2000; Gruss et al., 2001; Kufer et al., 2002; Tsai et al., 2003; Eyers and Maller, 2004; Groen et al., 2004). During interphase, however, TPX2 accumulates in the nucleus, and this nuclear accumulation of TPX2 could serve to stockpile functional protein for use during the next mitosis while preventing it from disturbing the interphase microtubule array. Alternatively, TPX2 could play a role in nuclear assembly or function.

The results reported here show for the first time that TPX2 plays a role during nuclear reformation after mitosis. Our most unexpected findings were that depletion of TPX2 from interphase *X. laevis* egg extracts severely affected nuclear size and that these effects appeared to be mediated through the interaction of TPX2 with the nuclear assembly protein LAP2. Surprisingly, depletion of TPX2 did not disrupt nuclear function, as TPX2-Δ nuclei were able to specifically import nuclear substrates and replicate their DNA. Indeed, in five out of seven independent experiments, TPX2-Δ nuclei replicated their DNA up to 2.5-fold more efficiently than mock-depleted controls. This increase in DNA replication efficiency is strikingly similar to the phenotype of "overexpressing" a human LAP2β truncation mutant encompassing the lamin and chromatin binding region (amino acids 1–408) in *X. laevis* egg extracts (Gant et al., 1999). These results are consistent with the idea that the concentrations of factors inside the nucleus, rather than nuclear structure by itself, are essential for replication competence (Walter et al., 1998), although we cannot yet rule out a direct role for TPX2 in regulating DNA replication.

Our finding that TPX2 depletion results in small nuclei is reminiscent of the results reported by Yang et al. (1997), who showed that microinjection of the lamin binding region of rat LAP2 strongly inhibited the threefold nuclear volume increase that takes place during early G1 in HeLa cells (Yang et al., 1997). Similarly, addition of a dominant-negative LAP2 mutant to *X. laevis* egg extracts resulted in membrane attachment and nuclear expansion defects (Gant et al., 1999).

Two possibilities exist to explain the observed nuclear morphology defects in TPX2-Δ nuclei: TPX2 could be required to regulate NE assembly (presumably through interaction with LAP2) or, alternatively, depletion of TPX2 could result in codepletion of LAP2 from the system. Two arguments suggest that the second possibility is less likely: (1) in extracts from which routinely >98% of TPX2 had been removed by immunodepletion, at least 90% of LAP2 remained in the extract (Fig. 4 B, d). More important, nuclear size could largely be rescued by readdition of bacterially expressed recombinant TPX2 alone. (2) Addition of exogenous TPX2 also disrupted nuclear morphology under conditions where the levels of LAP2 have not been altered. We therefore favor the hypothesis that TPX2 functions in NE assembly by regulating LAP2.

Our finding that LAP2 fails to accumulate in TPX2-Δ nuclei, whereas the localization of TPX2 is unaffected when LAP2 is disrupted, suggests that TPX2 might play a role in the targeting or perhaps anchoring of LAP2. Furthermore, the findings that both reduction and increase in the levels of TPX2 affect nuclear morphology and that TPX2 needs to be present during the early stages of nuclear reformation suggest that the stoichiometry of TPX2 and LAP2 during the early stages of nuclear assembly is important. In this context, it is interesting to note that TPX2 protein levels are tightly regulated during the cell cycle (Gruss et al., 2002; Stewart and Fang, 2005). Although recent studies showed that the bulk of TPX2 is degraded via the anaphase promoting complex/cyclosome and its activator Cdh1 (APC/C^{Cdh1}) after mitosis in HeLa cells (Stewart and Fang, 2005), analysis of individual cells (both the *X. laevis* tissue culture cells used here and HeLa cells; Stewart and Fang, 2005) shows that detectable levels of TPX2 are still present during telophase and cytokinesis, i.e., during the early stages of nuclear reformation. These results are consistent with the notion that TPX2 acts before the chromatin is enclosed in a NE (Fig. 1). Presumably, its degradation after nuclear enclosure has little consequence for nuclear assembly, although this hypothesis remains to be tested experimentally. Although the presence of TPX2 during nuclear reformation in tissue culture cells does not prove that TPX2 is required for this process, our findings are consistent with the idea that the involvement of TPX2 in nuclear reformation is not restricted to early embryos but may be a feature of somatic cells as well.

In summary, four lines of evidence lead us to propose that TPX2 regulates LAP2 function during nuclear assembly: (1) TPX2 interacts with LAP2 in vitro and during interphase but much less during mitosis, and both proteins localize to the nuclear rim; (2) the phenotypes of disrupting LAP2 or TPX2 are remarkably similar; (3) both TPX2 and LAP2 are required during the early stages of NE reformation; and (4) LAP2 distribution is disrupted in TPX2-Δ nuclei.

Perhaps our results can help provide an explanation for the different phenotypes observed upon TPX2 depletion from mitotic egg extracts (Wittmann et al., 2000), *X. laevis* tissue culture cells (Schatz et al., 2003), or human tissue culture cells (Garrett et al., 2002; Gruss et al., 2002), which included spindles with unfocused spindle poles, mitotic cells with two robust asters that are unable to assemble a spindle midzone, and a complete absence of microtubules. Depending on the amount of TPX2 that remains in the extracts or cells, it is possible that one or more of the observed phenotypes is a consequence of defects in nuclear assembly or growth after the previous cell division rather than a mitotic defect. We are currently exploring these possibilities further.

Materials and methods

Antibodies

TPX2 antibodies (diluted 1:1,000 for indirect immunofluorescence [IIF]) were raised in rabbits against full-length recombinant TPX2 protein and affinity purified (Tsai et al., 2003). For the depletion experiments, affinity-purified TPX2 antibodies were cross-linked to protein A beads as described previously (Harlow and Lane, 1988). Rabbit polyclonal antibodies against human LAP2β (2805; raised against amino acids 1–408 of human LAP2β; diluted 1:1,000 for IIF) or against *X. laevis* LAP2 (2807; raised against amino acids 1–165 of *X. laevis* LAP2; diluted 1:10,000 for Western blot) were provided by K. Wilson (Johns Hopkins Medical School, Baltimore, MD). Guinea pig polyclonal antibodies against *X. laevis* LAP2 (diluted 1:500 for IIF and 1:3,000 for Western blots) were described in Lang and

Krohne (2003). Monoclonal antibody L6-5D5, directed against *X. laevis* lamin B3 (Stick, 1988) were diluted 1:400 for IIF and were a gift from R. Stick (University of Bremen, Bremen, Germany) and Bob Goldman (Northwestern University, Chicago, IL). MAb414 antibodies were purchased from Covance and were diluted 1:5,000 for IIF. Alexa 488– or Alexa 594–conjugated secondary antibodies (1:1,000) were purchased from Invitrogen. Alkaline-phosphatase–linked secondary antibodies used for Western blots were purchased from Sigma-Aldrich.

Protein purification

X. laevis TPX2 fused to GST (using the vector pGEX-6P2 [GE Healthcare]; Tsai et al., 2003) was expressed in *Escherichia coli* strain MG1655 ΔKJ (a gift from E. Craig, University of Wisconsin–Madison, Madison, WI). This bacterial strain was used to express TPX2 because chaperones were a common contaminant in our TPX2 preparations and this strain lacks the heat shock proteins DnaJ and DnaK (Kang and Craig, 1990), thus yielding more highly purified TPX2. GST-TPX2 was purified on glutathione-agarose beads according to the manufacturer's instructions and either it was used directly (in the case of the pull-down experiments; Fig. 4) or the GST tag was removed from the protein (add-back experiments and in vitro interactions; Figs. 1, 4, and 6) by incubation with PreScission Protease (GE Healthcare) as described by the manufacturer. In either case, the protein was concentrated to ∼5 mg/ml, dialyzed overnight against XB buffer (10 mM K-Hepes, 100 mM KCl, 1 mM $MgCl_2$, 0.1 mM $CaCl_2$, and 50 mM sucrose, pH 7.6) supplemented with 1 mM DTT, and small aliquots were flash frozen in liquid nitrogen and stored at −80°C.

Human 6-His LAP2β (amino acids 1–408 of human LAP2β) was a gift from K. Wilson and was purified as described previously (Gant et al., 1999). The GST *X. laevis* LAP2β construct (amino acids 1–471 of *X. laevis* LAP2) was a gift from G. Krohne (University of Würzburg, Würzburg, Germany) and was purified on glutathione-agarose beads according to the manufacturer's instructions. The protein was concentrated to ∼5 mg/ml, dialyzed against XB buffer, flash frozen in small aliquots in liquid nitrogen, and stored at −80°C.

***X. laevis* egg extracts and TPX2 depletions**

Crude interphase nuclear assembly extracts were prepared as described previously (Newmeyer and Wilson, 1991) and were used fresh for all experiments except for the GST pull downs, for which extracts were prepared by cycling mitotic extracts (Murray, 1991; Desai et al., 1999) into interphase by the addition of 400 μM Ca^{2+}. To deplete extracts, 200 μl of freshly prepared crude extracts were incubated twice for 1 h each with 50 μl of Affi-Prep protein A beads (Bio-Rad Laboratories) cross-linked to antibodies (anti-TPX2 or nonimmune rabbit IgG) at 4°C. The beads were removed from the depleted extracts by a brief (10-s) centrifugation in a nanofuge.

Nuclear assembly reactions

Demembranated *X. laevis* sperm chromatin (1,000/microliter final; Murray, 1991) was added to 20 μl of extract on ice, and the reaction was moved to room temperature to initiate nuclear assembly. Reactions were incubated for 80 min unless otherwise indicated. For reconstitution experiments, purified TPX2 (without the GST tag) was added (100 nM final concentration) to extracts that were previously depleted of endogenous TPX2.

Probes for NE components

To visualize nuclear membranes, nuclear assembly reactions were spotted onto a microscope slide and mixed (2:1) with a solution containing 3.7% formaldehyde, 20 μg/ml bisbenzimide H33342 trihydrochloride fluorophore (Hoechst dye; Calbiochem), and 20 μg/ml DHCC ($DiOC_6$; Invitrogen) membrane dye in membrane wash buffer (MWB; 250 mM sucrose, 50 mM KCl, 2.5 mM $MgCl_2$, 50 mM Hepes, 1 mM DTT, 1 mM ATP, and 1 μg/ml LPC, pH 8.0). Nuclear membranes and DNA were visualized by fluorescence or by differential interference contrast microscopy, as indicated.

For immunofluorescence of in vitro–assembled nuclei, nuclear assembly reactions were incubated for 80 min (or the indicated times; Fig. 6) and processed as described by Mills et al. (1989), with the following modifications. 200 μl of fix solution (4% formaldehyde in nuclear wash buffer [200 mM sucrose, 50 mM KCl, 2.5 mM $MgCl_2$, 15 mM Hepes, pH 7.4, and 1 mM DTT]) was added to 20 μl of a nuclear assembly reaction, and the mixture was incubated for 10 min at 22–25°C. The mixture was layered over a 2-ml cushion of 30% sucrose in nuclear wash buffer in a glass tube (Corex) modified to hold a coverslip, as described by Mitchison and Kirschner (1986). The samples were then spun (3,400 rpm for 7 min at 4°C; JS13 rotor [Beckman Coulter]) onto poly-lysine–coated coverslips, and the coverslips were processed for immunofluorescence (mAb 414, lamin B3, or LAP2) as described (see Immunofluorescence and microscopy).

Nuclear import assays

Nucleoplasmin was purified from extracts and labeled with 5 (and 6) carboxytetramethylrhodamine succinimidyl ester ("tetramethylrhodamine"; Invitrogen) as described previously (Newmeyer and Wilson, 1991). Labeled nucleoplasmin was added to nuclear assembly reactions 60 min after initiating assembly, and the mixture was incubated for a further 20 min. A 2-μl reaction sample was then spotted onto a coverslip, fixed with 1 μl of 3.7% formaldehyde in MWB containing 20 μg/ml Hoechst dye, and viewed under the fluorescence microscope.

Dextran exclusion assays

The integrity of the NE membranes was visualized using dextran exclusion. 155-kD TRITC-dextran (0.1 mg/ml final; Sigma-Aldrich) was added to nuclear assembly reactions after 60 min of assembly, and the reactions were allowed to proceed for another 20 min. A 2-μl reaction sample was then spotted onto a coverslip, fixed with 1 μl of 3.7% formaldehyde in MWB containing 20 μg/ml Hoechst dye, and viewed in the fluorescence microscope.

TPX2 and LAP2 overexpression

For TPX2 overexpression, nuclear assembly reactions were supplemented with 0.2, 1.5, 2.5, 3.5, or 6.0 μM of recombinant TPX2 (without the GST) purified from bacteria. For LAP2 overexpression, reactions were supplemented with 3.0 μM bacterially expressed recombinant human LAP2β. Control reactions were supplemented with XB buffer. After incubation at 22–25°C for 80 min, the reactions were fixed in solution and spun onto poly-lysine–coated coverslips (described in Probes for NE components). Nuclear size was assessed based on DNA staining with Hoechst dye.

Immunofluorescence and microscopy

XLKWG cells were grown on coverslips (Martin et al., 1998), washed once with PBS, and fixed in 4% paraformaldehyde in PBS for 10 min. Nuclear assembly reactions were fixed in solution and spun onto polylysine–coated coverslips (described in Probes for NE components). For IIF, coverslips (of cells or nuclear assembly reactions) were washed with TBS-T (150 mM NaCl, 20 mM Tris-HCl, pH 7.4, and 0.1% Triton X-100), and nonspecific binding was blocked by incubation with Abdil (TBS-T plus 2% BSA and 0.1% sodium azide) for 40 min. Coverslips were then incubated with the appropriate primary and secondary antibodies (diluted in Abdil) for 1 h each in a humidified chamber at 22°C. To visualize DNA, coverslips were rinsed in water, dipped into a solution of 200 μg/ml Hoechst dye in water for 15 s, rinsed again in water, and mounted in mounting medium (Sigma-Aldrich). Samples were photographed with a cooled charge-coupled device camera (Photometrics CoolSnap HQ; Roper Scientific, Inc.) through a 60×/1.4 NA plan apo objective mounted on a fluorescence microscope (Eclipse E800; Nikon). Images were obtained using MetaMorph software and processed using Photoshop (Adobe).

EM

Samples were processed for EM by a modification of the procedure described by Macaulay and Forbes (1996). 50 μl of mock or TPX2-Δ nuclear assembly reactions were diluted in 500 μl of ice-cold MWB, the mixture was placed on ice, and 550 μl of EM fix (250 mM sucrose, 100 mM Hepes, pH 8.0, 1.5 mM $MgCl_2$, 1.5 mM $CaCl_2$, 1% glutaraldehyde, and 0.5% paraformaldehyde) was slowly added to the diluted nuclei. The reactions were incubated on ice for 1 h, and the nuclei were collected at top speed in a horizontal rotor for 3 min. The pellets were washed three times (10 min per wash) in 0.2 M cacodylate, pH 7.4, and were incubated in 1% OsO_4 buffered in 0.2 M cacodylate, pH 7.4, for 1 h on ice. The pellets were washed twice (5 min each) in ddH_2O and were stained overnight on ice with 1% uranyl acetate in ddH_2O. The pellets were dehydrated through a graded ethanol series (50, 75, 95, and 100% pure ethanol). Dehydrated pellets were embedded in Spurr's low viscosity medium (Ted Pella, Inc.) and hardened at 70°C for 20 h. Blocks were sectioned, poststained with 1% uranyl acetate and lead citrate, and viewed at 75 kV on an electron microscope (H-7000; Hitachi).

Nuclear size measurements

Nuclear area was measured using the trace region function of MetaMorph to outline individual nuclei. The area enclosed in the outlined region was measured using the region measurements function. At least 50 nuclei were measured per condition in each of five separate experiments. Standard deviations were calculated from the mean nuclear size for each experiment.

DNA replication assays

DNA replication was measured in seven independent experiments by incorporation of [^{32}P]dCTP (3,000 Ci/mmol; Redivue [GE Healthcare]) as described by Powers et al. (1995) with the following modifications: 20 μl of extract (TPX2-Δ, mock-depleted, or negative control extract) was supplemented with 1,000 sperm/microliter and 10 μCi of [^{32}P]dCTP and was incubated for 3 h at 22°C. Two types of negative controls were used with identical results: extract treated with 50 μM aphidicolin (Fisher Scientific) or mitotic extract. After addition of an equal amount of stop buffer (80 mM Tris-HCl, pH 8.0, 8 mM EDTA, 0.13% phosphoric acid, 10% Ficoll, 5% SDS, and 0.2% bromophenol blue) and proteinase K digestion (Powers et al., 1995), the samples were separated on a 0.8% agarose gel. Incorporation of label was detected by autoradiography of the wet gel using a PhosphorImager and was quantitated using Photoshop.

GST pull downs

To keep the conditions between mitotic and interphase pull downs as similar as possible, we prepared interphase extract from an aliquot of mitotic extract by the addition of 400 μM Ca^{2+}. GST-TPX2 pull downs from mitotic and interphase extracts were performed as described previously (O'Brien et al., 2005). In brief, GST-TPX2, GST alone, or buffer were added to extract and incubated at 4°C on a rotator. After 30 min, glutathione-agarose beads (Sigma-Aldrich) were added, and the mixture was incubated for an additional 60 min at 4°C. The beads were retrieved by a brief spin and washed, and bound proteins were eluted by digesting with PreScission protease. Eluted proteins were separated on 10% SDS-PAGE gels and visualized by staining with Coomassie stain or transferred to nitrocellulose and Western blotted according to standard protocols.

Immunoprecipitations

To immunoprecipitate TPX2 or LAP2, 100 μl of freshly prepared crude extracts were incubated for 1 h at 4°C with antibodies covalently cross-linked to Affi-Prep protein A beads. Antibodies used were rabbit anti-TPX2, guinea pig anti–*X. laevis* LAP2, or rabbit IgG against an irrelevant antigen (maskin; O'Brien et al., 2005). The beads were collected by a brief (10-s) centrifugation in a nanofuge, washed three times with HB (50 mM Hepes, 1 mM EGTA, and 1 mM $MgCl_2$, pH 7.6) plus 100 mM NaCl and once in HB plus 250 mM NaCl. The beads were then resuspended in 25 μl of 2× SDS sample buffer and boiled. Equal fractions of each sample were then separated by 10% SDS-PAGE, transferred to nitrocellulose, and Western blotted according to standard protocols.

Mass spectrometry

GST-TPX2 pull downs were concentrated and separated on a 10% gel. Gel bands were excised from the gel and prepared as described previously (http://www.biotech.wisc.edu/ServicesResearch/MassSpec/ingel.htm). MALDI-TOF mass spectrometry was performed by facility staff on a matrix-assisted laser desorption ionization–time of flight instrument (BIFLEX III; Bruker Daltonics).

In vitro binding assays

Increasing amounts of bacterially expressed purified recombinant TPX2 (without the GST tag) were combined with 3.6 μM of bacterially expressed purified GST–*X. laevis* LAP2 in a test tube in a total volume of 50 μl. Molar ratios of LAP2/TPX2 were 5:1, 2.5:1, 1:1, 1:2.5, and 1:5. A control reaction contained 3.6 μM of TPX2 but no GST-LAP2. 25 μl of GST-agarose beads were added to each binding reaction, and reactions were incubated for 1 h at 4°C with rotation. The beads were collected by brief centrifugation in a nanofuge, the supernatant was collected, and the beads were washed three times with HB plus 100 mM NaCl and once with 0.1% Triton X-100 in HB plus 250 mM NaCl. Proteins were eluted from the beads by boiling in SDS sample buffer. 4× SDS sample buffer was added to the supernatant to 1×. 20 μl of the beads or 30 μl of supernatant were separated by 10% SDS-PAGE. The gel was stained with Coomassie to visualize protein.

Sperm chromatin decondensation assay

Chromatin decondensation was assayed as described by Philpott et al. (1991), with the following modifications: 20 μl of untreated, mock-depleted, or TPX2-Δ *X. laevis* interphase extract high-speed supernatant (prepared as described by Newmeyer and Wilson [1991]) was supplemented with ~1,000 sperm/microliter and incubated at 22°C. 1, 5, 10, 30, and 60 min after initiation of the reaction, 2-μl samples were spotted onto a coverslip, fixed with 1 μl of 3.7% formaldehyde in MWB containing 20 μg/ml Hoechst dye, and viewed in the fluorescence microscope. As a control, sperm chromatin not incubated in extract was spotted directly onto a slide, fixed, and viewed.

Online supplemental material

Fig. S1 shows the results of the sperm chromatin decondensation assay. Fig. S2 shows nuclei assembled in TPX2 or mock-depleted extracts fixed at various time points and stained with mAb414 or antibodies to lamin B3. Fig. S3 shows higher magnification micrographs of selected images from Fig. 6. Online supplemental material is available at http://www.jcb.org/cgi/content/full/jcb.200512107/DC1.

We thank Dr. Carol Sattler (McArdle Laboratory, University of Wisconsin–Madison) for expert EM assistance; Drs. Kathy Wilson, Georg Krohne, Betty Craig, Bob Goldman, and Reimer Stick for sharing antibodies, constructs, and/or reagents; and Dr. Dale Shumaker (Northwestern University Feinberg School of Medicine, Chicago, IL) and members of the Wiese laboratory for critical reading of the manuscript.

This work was supported by National Science Foundation grant MCB-0344723. Work in the Wiese laboratory was also supported by a Kimmel Scholar Award (to C. Wiese) from the Sidney Kimmel Foundation for Cancer Research and start-up funds from the University of Wisconsin–Madison Graduate School, the College of Agricultural and Life Sciences, and the Department of Biochemistry.

Submitted: 20 December 2005
Accepted: 1 May 2006

References

Alsheimer, M., E. Fecher, and R. Benavente. 1998. Nuclear envelope remodeling during rat spermiogenesis: distribution and expression pattern of LAP2/thymopoietins. *J. Cell Sci.* 111:2227–2234.

Askjaer, P., V. Galy, E. Hannak, and I.W. Mattaj. 2002. Ran GTPase cycle and importins alpha and beta are essential for spindle formation and nuclear envelope assembly in living *Caenorhabditis elegans* embryos. *Mol. Biol. Cell.* 13:4355–4370.

Berger, R., L. Theodor, J. Shoham, E. Gokkel, F. Brok-Simoni, K.B. Avraham, N.G. Copeland, N.A. Jenkins, G. Rechavi, and A.J. Simon. 1996. The characterization and localization of the mouse thymopoietin/lamina-associated polypeptide 2 gene and its alternatively spliced products. *Genome Res.* 6:361–370.

Boman, A.L., M.R. Delannoy, and K.L. Wilson. 1992. GTP hydrolysis is required for vesicle fusion during nuclear envelope assembly in vitro. *J. Cell Biol.* 116:281–294.

Davis, L.I., and G. Blobel. 1986. Identification and characterization of a nuclear pore complex protein. *Cell.* 45:699–709.

Dechat, T., J. Gotzmann, A. Stockinger, C.A. Harris, M.A. Talle, J.J. Siekierka, and R. Foisner. 1998. Detergent-salt resistance of LAP2α in interphase nuclei and phosphorylation-dependent association with chromosomes early in nuclear assembly implies functions in nuclear structure dynamics. *EMBO J.* 17:4887–4902.

Dechat, T., S. Vlcek, and R. Foisner. 2000. Lamina-associated polypeptide 2 isoforms and related proteins in cell cycle-dependent nuclear structure dynamics. *J. Struct. Biol.* 129:335–345.

Desai, A., A. Murray, T.J. Mitchison, and C.E. Walczak. 1999. The use of *Xenopus* egg extracts to study mitotic spindle assembly and function *in vitro*. *Methods Cell Biol.* 61:385–412.

Di Fiore, B., M. Ciciarello, and P. Lavia. 2004. Mitotic functions of the Ran GTPase network: the importance of being in the right place at the right time. *Cell Cycle.* 3:305–313.

Eyers, P.A., and J.L. Maller. 2004. Regulation of *Xenopus* Aurora A activation by TPX2. *J. Biol. Chem.* 279:9008–9015.

Finlay, D.R., D.D. Newmeyer, T.M. Price, and D.J. Forbes. 1987. Inhibition of *in vitro* nuclear transport by a lectin that binds to nuclear pores. *J. Cell Biol.* 104:189–200.

Foisner, R., and L. Gerace. 1993. Integral membrane proteins of the nuclear envelope interact with lamins and chromosomes, and binding is modulated by mitotic phosphorylation. *Cell.* 73:1267–1279.

Furukawa, K., N. Pante, U. Aebi, and L. Gerace. 1995. Cloning of a cDNA for lamina-associated polypeptide 2 (LAP2) and identification of regions that specify targeting to the nuclear envelope. *EMBO J.* 14:1626–1636.

Furukawa, K., C.E. Fritze, and L. Gerace. 1998. The major nuclear envelope targeting domain of LAP2 coincides with its lamin binding region but is distinct from its chromatin interaction domain. *J. Biol. Chem.* 273:4213–4219.

Gant, T.M., and K.L. Wilson. 1997. Nuclear assembly. *Annu. Rev. Cell Dev. Biol.* 13:669–695.

Gant, T.M., C.A. Harris, and K.L. Wilson. 1999. Roles of LAP2 proteins in nuclear assembly and DNA replication: truncated LAP2β proteins alter

lamina assembly, envelope formation, nuclear size, and DNA replication efficiency in *Xenopus laevis* extracts. *J. Cell Biol.* 144:1083–1096.

Garrett, S., K. Auer, D.A. Compton, and T.M. Kapoor. 2002. hTPX2 is required for normal spindle morphology and centrosome integrity during vertebrate cell division. *Curr. Biol.* 12:2055–2059.

Gerace, L., and G. Blobel. 1980. The nuclear envelope lamina is reversibly depolymerized during mitosis. *Cell.* 19:277–287.

Goldberg, M., E. Nili, G. Cojocaru, Y.B. Tzur, R. Berger, M. Brandies, G. Rechavi, Y. Gruenbaum, and A.J. Simon. 1999. Functional organization of the nuclear lamina. *Gene Ther. Mol. Biol.* 4:143–158.

Goldman, R.D., Y. Gruenbaum, R.D. Moir, D.K. Shumaker, and T.P. Spann. 2002. Nuclear lamins: building blocks of nuclear architecture. *Genes Dev.* 16:533–547.

Groen, A.C., L.A. Cameron, M. Coughlin, D.T. Miyamoto, T.J. Mitchison, and R. Ohi. 2004. XRHAMM functions in Ran-dependent microtubule nucleation and pole formation during anastral spindle assembly. *Curr. Biol.* 14:1801–1811.

Gruenbaum, Y., R.D. Goldman, R. Meyuhas, E. Mills, A. Margalit, A. Fridkin, Y. Dayani, M. Prokocimer, and A. Enosh. 2003. The nuclear lamina and its functions in the nucleus. *Int. Rev. Cytol.* 226:1–62.

Gruenbaum, Y., A. Margalit, R.D. Goldman, D.K. Shumaker, and K.L. Wilson. 2005. The nuclear lamina comes of age. *Nat. Rev. Mol. Cell Biol.* 6:21–31.

Gruss, O.J., and I. Vernos. 2004. The mechanism of spindle assembly: functions of Ran and its target TPX2. *J. Cell Biol.* 166:949–955.

Gruss, O.J., R.E. Carazo-Salas, C.A. Schatz, G. Guarguaglini, J. Kast, M. Wilm, N. Le Bot, I. Vernos, E. Karsenti, and I.W. Mattaj. 2001. Ran induces spindle assembly by reversing the inhibitory effect of importin alpha on TPX2 activity. *Cell.* 104:83–93.

Gruss, O.J., M. Wittmann, H. Yokoyama, R. Pepperkok, T. Kufer, H. Sillje, E. Karsenti, I.W. Mattaj, and I. Vernos. 2002. Chromosome-induced microtubule assembly mediated by TPX2 is required for spindle formation in HeLa cells. *Nat. Cell Biol.* 4:871–879.

Hachet, V., T. Köcher, M. Wilm, and I.W. Mattaj. 2004. Importin α associates with membranes and participates in nuclear envelope assembly *in vitro*. *EMBO J.* 23:1526–1535.

Harel, A., R.C. Chan, A. Lachish-Zalait, E. Zimmerman, M. Elbaum, and D.J. Forbes. 2003. Importin β negatively regulates nuclear membrane fusion and nuclear pore complex assembly. *Mol. Biol. Cell.* 14:4387–4396.

Harlow, E., and D. Lane. 1988. *Antibodies: A Laboratory Manual*. Cold Spring Harbor Laboratory, Cold Spring Harbor, NY. 353 pp.

Harris, C.A., P.J. Andryuk, S.C. Cline, A. Natarajan, J.J. Siekierka, and G. Goldstein. 1994. Three distinct human thymopoietins are derived from alternatively spliced mRNAs. *Proc. Natl. Acad. Sci. USA.* 91:6283–6287.

Harris, C.A., P.J. Andryuk, S.W. Cline, S. Mathew, J.J. Siekierka, and G. Goldstein. 1995. Structure and mapping of the human thymopoietin (TMPO) gene and relationship of human TMPO beta to rat lamin-associated polypeptide 2. *Genomics.* 28:198–205.

Hetzer, M., T.C. Walther, and I.W. Mattaj. 2005. Pushing the envelope: structure, function, and dynamics of the nuclear periphery. *Annu. Rev. Cell Dev. Biol.* 21:347–380.

Holmer, L., and H.J. Worman. 2001. Inner nuclear membrane proteins: functions and targeting. *Cell. Mol. Life Sci.* 58:1741–1747.

Ishijima, Y., T. Toda, H. Matsushita, M. Yoshida, and N. Kimura. 1996. Expression of thymopoietin beta/lamina-associated polypeptide 2 (TP beta/LAP2) and its family proteins as revealed by specific antibody induced against recombinant human thymopoietin. *Biochem. Biophys. Res. Commun.* 226:431–438.

Kang, P.J., and E.A. Craig. 1990. Identification and characterization of a new *Escherichia coli* gene that is a dosage-dependent suppressor of a dnaK deletion mutation. *J. Bacteriol.* 172:2055–2064.

Kline-Smith, S.L., and C.E. Walczak. 2004. Mitotic spindle assembly and chromosome segregation: refocusing on microtubule dynamics. *Mol. Cell.* 15:317–327.

Kufer, T.A., H.H.W. Sillje, R. Körner, O.J. Gruss, P. Meraldi, and E.A. Nigg. 2002. Human TPX2 is required for targeting Aurora-A kinase to the spindle. *J. Cell Biol.* 158:617–623.

Lang, C., and G. Krohne. 2003. Lamina-associated polypeptide 2beta (LAP2beta) is contained in a protein complex together with A- and B-type lamins. *Eur. J. Cell Biol.* 82:143–153.

Lang, C., M. Paulin-Levasseur, A. Gajewski, M. Alsheimer, R. Benavente, and G. Krohne. 1999. Molecular characterization and developmentally regulated expression of *Xenopus* lamina-associated polypeptide 2 (XLAP2). *J. Cell Sci.* 112:749–759.

Lopez-Soler, R.I., R.D. Moir, T.P. Spann, R. Stick, and R.D. Goldman. 2001. A role for nuclear lamins in nuclear envelope assembly. *J. Cell Biol.* 154:61–70.

Macaulay, C., and D.J. Forbes. 1996. Assembly of the nuclear pore: biochemically distinct steps revealed with NEM, GTP γ S, and BAPTA. *J. Cell Biol.* 132:5–20.

Maidment, S.L., and J.A. Ellis. 2002. Muscular dystrophies, dilated cardiomyopathy, lipodystrophy and neuropathy: the nuclear connection. *Expert Rev. Mol. Med.* 2002:1–21.

Marshall, I.C.B., and K.L. Wilson. 1997. Nuclear envelope assembly after mitosis. *Trends Cell Biol.* 7:69–74.

Martin, O.C., R.N. Gunawardane, A. Iwamatsu, and Y. Zheng. 1998. Xgrip109: A γ tubulin-associated protein with an essential role in γ tubulin ring complex (γTuRC) assembly and centrosome function. *J. Cell Biol.* 141:675–687.

Mills, A.D., J.J. Blow, J.G. White, W.B. Amos, D. Wilcock, and R.A. Laskey. 1989. Replication occurs at discrete foci spaced throughout nuclei replicating *in vitro*. *J. Cell Sci.* 94:471–477.

Mitchison, T.J., and M.W. Kirschner. 1986. Isolation of mammalian centrosomes. *Methods Enzymol.* 134:261–268.

Murray, A.W. 1991. Cell cycle extracts. *Methods Cell Biol.* 36:581–605.

Newmeyer, D.D., and K.L. Wilson. 1991. Egg extracts for nuclear import and nuclear assembly reactions. *Methods Cell Biol.* 36:607–634.

Newport, J.W., K.L. Wilson, and W.G. Dunphy. 1990. A lamin-independent pathway for nuclear envelope assembly. *J. Cell Biol.* 111:2247–2259.

O'Brien, L.L., A.J. Albee, L. Liu, W. Tao, P. Dobrzyn, S.B. Lizarraga, and C. Wiese. 2005. The *Xenopus* TACC homologue, maskin, functions in mitotic spindle assembly. *Mol. Biol. Cell.* 16:2836–2847.

Philpott, A., G.H. Leno, and R.A. Laskey. 1991. Sperm decondensation in *Xenopus* egg cytoplasm is mediated by nucleoplasmin. *Cell.* 65:569–578.

Powers, M.A., C. Macaulay, F. Masiarz, and D.J. Forbes. 1995. Reconstituted nuclei depleted of a vertebrate GLFG nuclear pore protein, p97, import but are defective in nuclear growth and replication. *J. Cell Biol.* 128:721–736.

Quimby, B.B., and M. Dasso. 2003. The small GTPase Ran: interpreting the signs. *Curr. Opin. Cell Biol.* 15:338–344.

Ryan, K.J., J.M. McCaffery, and S.R. Wente. 2003. The Ran GTPase cycle is required for yeast nuclear pore complex assembly. *J. Cell Biol.* 160:1041–1053.

Schatz, C.A., R. Santarella, A. Hoenger, E. Karsenti, I.W. Mattaj, O.J. Gruss, and R.E. Carazo-Salas. 2003. Importin alpha-regulated nucleation of microtubules by TPX2. *EMBO J.* 22:2060–2070.

Schirmer, E.C., and L. Gerace. 2005. The nuclear membrane proteome: extending the envelope. *Trends Biochem. Sci.* 30:551–558.

Schirmer, E.C., L. Florens, T. Guan, J.R. Yates III, and L. Gerace. 2003. Nuclear membrane proteins with potential disease links found by subtractive proteomics. *Science.* 301:1380–1382.

Shumaker, D.K., E.R. Kuczmarski, and R.D. Goldman. 2003. The nucleoskeleton: lamins and actin are major players in essential nuclear functions. *Curr. Opin. Cell Biol.* 15:358–366.

Shumaker, D.K., R.I. Lopez-Soler, S.A. Adam, H. Herrmann, R.D. Moir, T.P. Spann, and R.D. Goldman. 2005. Functions and dysfunctions of the nuclear lamin Ig-fold domain in nuclear assembly, growth, and Emery-Dreifuss muscular dystrophy. *Proc. Natl. Acad. Sci. USA.* 102:15494–15499.

Stewart, S., and G. Fang. 2005. Anaphase-promoting complex/cyclosome controls the stability of TPX2 during mitotic exit. *Mol. Cell. Biol.* 25:10516–10527.

Stick, R. 1988. cDNA cloning of the developmentally regulated lamin LIII of *Xenopus laevis*. *EMBO J.* 7:3189–3197.

Theodor, L., J. Shoham, R. Berger, E. Gokkel, L. Trachtenbrot, A.J. Simon, F. Brok-Simon, U. Nir, E. Ilan, D. Zevin-Sonkin, et al. 1997. Ubiquitous expression of a cloned murine thymopoietin cDNA. *Acta Haematol.* 97:153–163.

Tsai, M., C. Wiese, K. Cao, O. Martin, P. Donovan, J. Ruderman, C. Prigent, and Y. Zheng. 2003. A Ran signaling pathway mediated by the mitotic kinase Aurora A in spindle assembly. *Nat. Cell Biol.* 5:242–248.

Walter, J., L. Sun, and J.W. Newport. 1998. Regulated chromosomal DNA replication in the absence of a nucleus. *Mol. Cell.* 1:519–529.

Walther, T.C., P. Askjaer, M. Gentzel, A. Habermann, G. Griffiths, M. Wilm, I.W. Mattaj, and M. Hetzer. 2003. RanGTP mediates nuclear pore complex assembly. *Nature.* 424:689–694.

Wittmann, T., M. Wilm, E. Karsenti, and I. Vernos. 2000. TPX2, a novel *Xenopus* MAP involved in spindle pole organization. *J. Cell Biol.* 149:1405–1418.

Yang, L., T. Guan, and L. Gerace. 1997. Lamin-binding fragment of LAP2 inhibits increase in nuclear volume during the cell cycle and progression into S-phase. *J. Cell Biol.* 139:1077–1087.

Zevin-Sonkin, D., E. Ilan, D. Guthmann, J. Riss, L. Theodor, and J. Shoham. 1992. Molecular cloning of the bovine thymopoietin gene and its expression in different calf tissues: evidence for a predominant expression in thymocytes. *Immunol. Lett.* 31:301–309.